optica

Speckle correlation resolution enhancement of wide-field fluorescence imaging: supplementary material

HASAN YILMAZ[1,*], ELBERT G. VAN PUTTEN[1,2], JACOPO BERTOLOTTI[1,3], AD LAGENDIJK[1], WILLEM L. VOS[1], AND ALLARD P. MOSK[1]

[1]Complex Photonic Systems (COPS), MESA+ Institute for Nanotechnology, University of Twente, P.O. Box 217, 7500 AE Enschede, The Netherlands
[2]Present address: Philips Research Laboratories, 5656 AE Eindhoven, The Netherlands
[3]Present address: Physics and Astronomy Department, University of Exeter, Stocker Road, Exeter EX4 4QL, United Kingdom
[*]Corresponding author: h.yilmaz@utwente.nl

Published 24 April 2015

This document provides supplementary information to "Speckle correlation resolution enhancement of wide-field fluorescence imaging," http://dx.doi.org/10.1364/optica.2.000424. We describe the details of our experimental and data analysis methods, as well as the sample preparation and the experimental set-up. We describe the new phase retrieval algorithm, convergence properties of the algorithm, and the inverse apodization procedure that we have developed. We describe the effective object size and the effective scattering lens NA estimation that yields the resolution of our experimental results. In the last section, we describe and present the information-theoretical analysis of our method and compare it to a similar method.

http://dx.doi.org/10.1364/optica.2.000424.s001

1. SAMPLE AND EXPERIMENTAL SETUP

We prepared a GaP scattering lens containing a low density of dye doped fluorescent nanospheres in the object plane. A porous layer with a thickness of 2 μm is prepared by electrochemical etching. The polished side of the GaP substrate is coated with 100 nm silicon (Si) layer by chemical vapour deposition to minimize internal reflections in the GaP lens that reduce the effective range of the optical memory effect. Dye-doped polystyrene nanospheres are drop-casted on a 10 μm-scale window of the Si coating side. Nanospheres have a diameter of 100 nm and have their absorption peak at 542 nm and emission peak at 612 nm.

The details of the experimental setup is shown in Fig. S1. The light source is a diode pumped solid state laser (Cobolt Jive, 100 mW continuous wave at 561 nm). We use a phase only spatial light modulator (Hamamatsu X10468-04) in the illumination path to generate a parabolic phase correction required for a proper displacement of the scattered light inside the GaP scattering lens [1]. The spatial light modulator is imaged onto a two-axis steering mirror and another lens and a microscope objective (Nikon: 20×, NA = 0.45) then demagnify the plane of the two-axis mirror onto the porous surface of the GaP substrate. An air microscope objective (Zeiss: Infinity corrected, 63×, NA = 0.95) images the object plane of the GaP substrate onto an EMCCD camera (Andor Luca DL-658M). Multiple band-pass filters (Semrock FF01-620/52-25) in front of the camera ensure that only the fluorescence light is detected.

2. THE GERCHBERG-SAXTON-TYPE ALGORITHM

We have developed a Gerchberg-Saxton-type (GS) algorithm for phase retrieval. Our Gerchberg-Saxton-type algorithm is shown by a block diagram in Fig. S2. We use the following procedure to retrieve the phase information of high-frequency Fourier components. As an initial guess, we use the standard resolution sub-image. The "Hybrid Input-Output" [2] algorithm is employed for β ranging from 2 to 0 in steps of 0.1. For each value of β the algorithm runs 10 iterations. Finally, 100 iterations with the "Error-Reduction" [2] algorithm are used to obtain convergence with a minimal error. In each iteration, we apply a high-pass filter to the retrieved phase and combine it with the low-pass filtered phase of the standard resolution sub-image. Low spatial frequency phase information of the standard resolution image eliminates ambiguities such as flips and translations of the object and satisfies a unique solution.

Typically, a Gerchberg-Saxton-type algorithm converges with

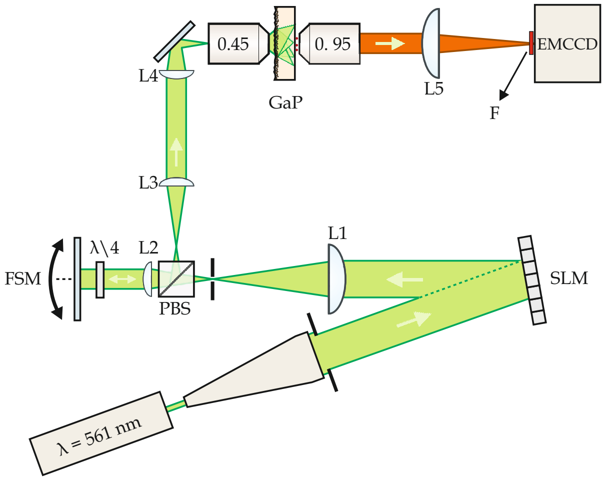

Fig. S1. Experimental setup: An expanded CW laser at 561 nm illuminates a spatial light modulator (SLM). The beam size on the SLM is 0.8 cm. The 0th order diffracted beam is imaged on a two-axis steering mirror. The 90° polarized beam is reflected from a polarizing beam splitter (PBS) is imaged on the scattering surface of the GaP wafer. The fluorescence from nanoparticles on the back side of the GaP wafer is imaged on an EMCCD camera. $\lambda/4$ is a quarter wave plate, and L1, L2, L3, L4, L5, lenses with a focal distance of 200 mm, 100 mm, 100 mm, 50 mm, and 500 mm, respectively.

about 1000 iterations that take in the order of a second with a modern computer. Our new Gerchberg-Saxton-type algorithm uses low-frequency phase of the Fourier components of the object as extra information. In our case, only 300 iterations are already sufficient. We apply this procedure to 2500 sub-images to obtain the high overlap, therefore the complete reconstruction takes about 20 minutes. The time scale of the reconstruction is independent of the resolution, while it follows a square law with respect to the ratio of the field-of-view and the speckle-scan range. In addition, the algorithm is very easy to parallelize and can run on a graphic card, ideally speeding it up by an order of magnitude.

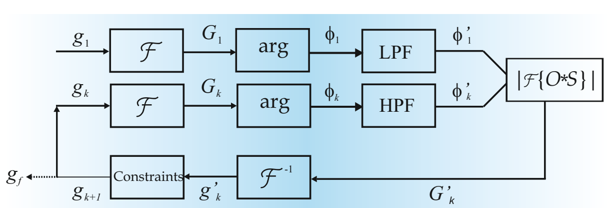

Fig. S2. Block diagram of our Gerchberg-Saxton-type algorithm: g_1: Initial guess; $\mathcal{F}$: Fourier transform; arg: Argument; LPF: Low-pass filter; HPF: High-pass filter; $|\mathcal{F}\{O * S\}|$: Magnitude of the measured spatial spectrum of the object O; $\mathcal{F}^{-1}$: Inverse Fourier transform; Constraints: Real domain constraints to calculate g_{k+1} out of g_k.

3. CONVERGENCE PROPERTIES OF THE GERCHBERG-SAXTON-TYPE ALGORITHM

To test the convergence properties of our modified GS algorithm on more complex objects we used a numerical test object composed of six letters on a white background (Fig. S3). We sim-

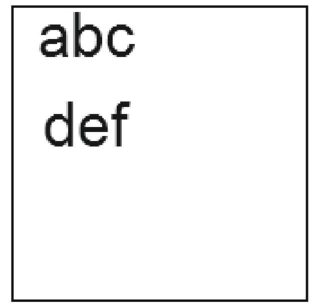

Fig. S3. The numerical test object: The numerical test object consisting of 6 letters on a 164 × 164 pixel canvas.

ulated the low-resolution imaging by Fourier filtering the object with an NA that was between about 1% and 15% of the full bandwidth of the object. Examples at an NA ratio $(\mathrm{NA}_{\mathrm{det}}/\mathrm{NA}_{\mathrm{ill}})$ of 0.05, 0.10 and 0.15 are given in Fig. S4.

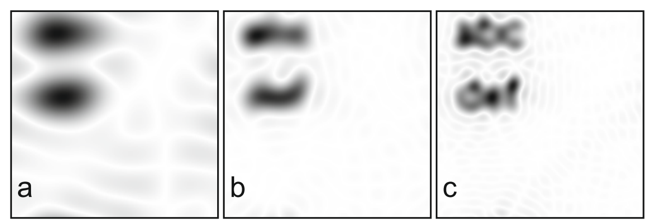

Fig. S4. Low-resolution images: Low-resolution images of the numerical object as used as input to the algorithm at an NA ratio of (a) 0.05; (b) 0.10; (c) 0.15.

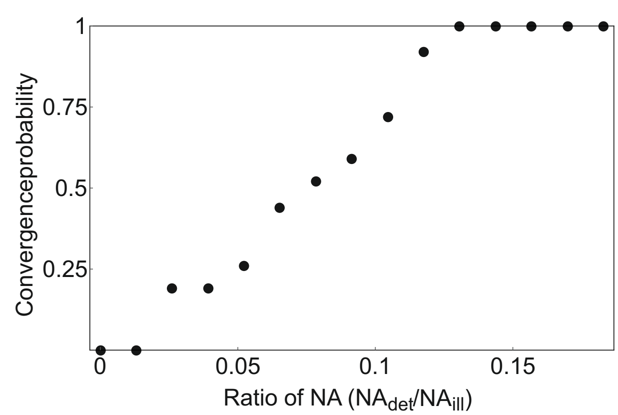

Fig. S5. Convergence rate: Convergence rate (out of 100 runs seeded with noise as an initial guess) for 6000 steps of our modified GS algorithm, versus NA ratio.

We ran 6000 steps of our modified GS algorithm to reconstruct the object from the low-resolution image plus the high-resolution autocorrelate. The probability of convergence after 6000 steps is shown versus NA ratio in Fig. S5, where we consider the algorithm as converged if the error drops below 1%. An example of a converged and non-converged run are given in Fig. S6. In 100 runs we found the algorithm never converged within 6000 steps for the lowest ratios (up to 0.03) and always converged for ratios greater than 0.13.

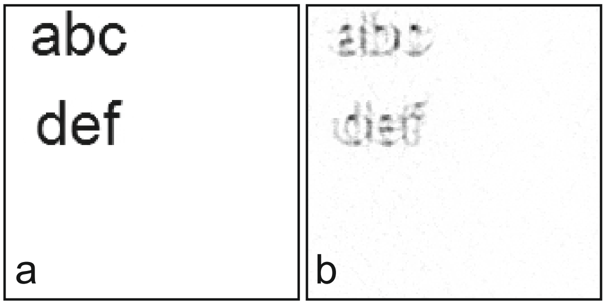

Fig. S6. Retrieved images: Example of the images retrieved by (a) a converged run and (b) a non-converged run, at a NA ratio of 0.07.

4. INVERSE APODIZATION

In incoherent imaging, optical transfer function of a circular aperture is approximately a cone-shaped function that results in suppression of the high-frequency Fourier components [3]. In our experimental demonstration, both the optical transfer functions of GaP scattering lens and of the detection objective are approximately cone-shaped functions with cut-off spatial frequencies of $k_{\text{ill}} = 27$ µm^{-1} and $k_{\text{det}} = 9.75$ µm^{-1} respectively. We have inverse apodized both wide-field conventional and SCORE images by dividing Fourier spectra of the wide-field SCORE image and the wide-field conventional image with corresponding inverse apodization functions (see Fig. S7).

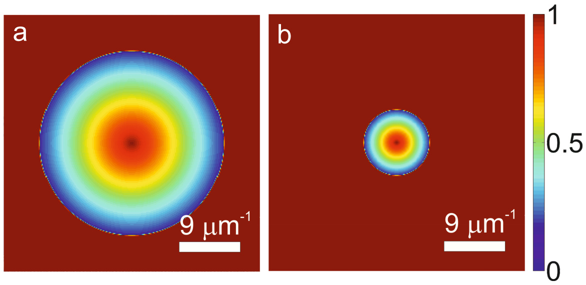

Fig. S7. Inverse apodization functions: (a) The inverse apodization function of the GaP scattering lens used for the wide-field SCORE image . (b) The inverse apodization function of the collection objective with NA = 0.95 used for the wide-field conventional image.

We used inverse apodization after the reconstruction of the SCORE image, because inverse apodization before the reconstruction affects the positivity of the fluorescence images which makes the reconstruction procedure impossible. We choose the cut-off frequency of our apodization function carefully in order to have minimal artefacts on the final wide-field SCORE image.

5. ESTIMATION OF THE OBJECT SIZE AND THE EFFECTIVE NA

In order to estimate the resolution of SCORE results, we deconvolve a SCORE image of a single nanosphere with the known size and shape of the object. In our experiment, we use polystyrene nanospheres with a diameter of 100 nm. Our nanospheres are positioned on the interface between the high-index GaP substrate and the low-index air as shown in Fig. S8. Incident light intensity at angles larger than the critical angle ($\theta_c = 17°$) at the interface will be totally internally reflected. However, the incident light will excite the fluorophores in the nanosphere via evanescent wave of the light. The decay length of the evanescent wave intensity depends on the angle of incidence on the interface as shown in Eq. S1. The decay length l of the evanescent wave intensity is

$$l(\theta) = \frac{1}{2k\sqrt{n^2 \sin^2\theta - 1}} \qquad \textbf{(S1)}$$

where k is the vacuum wavenumber of the incident light, n the

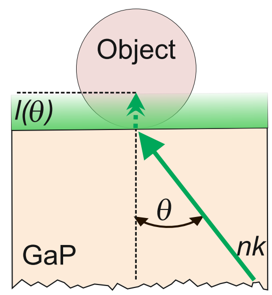

Fig. S8. Excitation of the fluorophores via evanescent wave: Light of a particular angle $\theta > \theta_c$ excites fluorophores that are buried inside a polystyrene nanosphere. The effective size of the nanosphere is different for each angle of incidence of light, since the decay length l is different for each angle of incidence of light.

refractive index of the GaP substrate, and θ the internal angle of the incident light on the interface [4]. We take the highest wave vector into consideration, since the highest wave vector determines the resolution. The decay length for the highest wave vector is $l = 20$ nm. The effective size of a spherical object on the interface will be a Gaussian-shaped object with a full-width-half-maximum of $\Delta_{\text{object}} = 70$ nm. In our SCORE images, a single image of a nanosphere has a full-width-half-maximum of $\Delta_{\text{feature}} = 135$ nm. Therefore we can use the formula to obtain our deconvolved PSF as $\Delta_{\text{PSF}} = (\Delta^2_{\text{feature}} - \Delta^2_{\text{object}})^{1/2} = 116$ nm corresponding to an effective NA = 2.4.

6. INFORMATION-THEORETICAL ANALYSIS

In this section, we present an information-theoretical bound on the signal-to-noise ratio of our method and a similar method (blind-SIM). Here, we show how the maximum achievable signal-to-noise ratio of SCORE and blind-SIM images scale with respect to the ratio of the illumination NA and the detection NA ($\text{NA}_{\text{ill}}/\text{NA}_{\text{det}}$).

The information capacity of one degree of freedom of an image is given by

$$H = \frac{1}{2}\log_2(SNR + 1) \qquad \textbf{(S2)}$$

where signal-to-noise ratio (SNR) is in optical power domain [5]. The information capacity for all degrees of freedom (diffraction-limited spots) of a detected intensity image is

$$H = \sum_{f=1}^{M} \frac{1}{2} \log_2(SNR + 1) \tag{S3}$$

where M is the total number of diffraction-limited spots [5].

We assume the noise is uncorrelated between diffraction-limited spots. The autocorrelation has a higher background compared to a standard resolution image and the signal-to-noise ratio drops at high NA ratios due to the finite dynamic range of the detection. Therefore the information capacity of the measured data of SCORE consisting of N frames of p^2 degrees of freedom is given by

$$H_{\text{in}} = \frac{1}{2} N p^2 \log_2(SNR_{\text{ac}} + 1) \tag{S4}$$

$$SNR_{\text{ac}} = \frac{SNR_{\text{in}} p}{q} \tag{S5}$$

where SNR_{ac} is the signal-to-noise ratio of the autocorrelation of the speckle-scan matrix, SNR_{in} the signal-to-noise ratio of a single wide-field image, and q^2 the number of illumination speckle grains in a single wide-field image. Our SCORE algorithm outputs a wide-field image with a resolution of the speckle grain size, and also recovers the illumination speckle pattern, so that the total number of degrees of freedom is $2q^2$. The information capacity of the output data of SCORE is given by

$$H_{\text{out}} = \frac{1}{2} 2q^2 \log_2(SNR_{\text{out}} + 1) \tag{S6}$$

where SNR_{out} is the signal-to-noise ratio of the reconstructed SCORE image. The fact that the output cannot contain more information than the input results in

$$H_{\text{out}}^{\text{max}} = H_{\text{in}} \tag{S7}$$

$$N p^2 \log_2\left(\frac{SNR_{\text{in}} p}{q} + 1\right) = 2q^2 \log_2(SNR_{\text{out}}^{\text{max}} + 1). \tag{S8}$$

The number of uncorrelated measurements is $N = q^2/p^2$ assuming our scan area is equal to a diffraction-limited spot of the imaging results in

$$SNR_{\text{out}}^{\text{max}} = \sqrt{\frac{SNR_{\text{in}} p}{q} + 1} - 1. \tag{S9}$$

Here it is evident that as the illumination NA becomes higher compared to the detection NA, the $SNR_{\text{out}}^{\text{max}}$ drops.

Now we turn to information-theoretical analysis of the blind-SIM method. Information capacity of the measured data of blind-SIM is given by

$$H_{\text{in}} = \frac{1}{2} N p^2 \log_2(SNR_{\text{in}} + 1). \tag{S10}$$

Blind-SIM requires illumination of the object with N uncorrelated and different speckle patterns. In essence, this method reconstructs a high-resolution fluorescence image of the object as well as N illuminating high-resolution images of the speckle patterns by a blind-deconvolution-based algorithm with a total number of degrees of freedom of $Nq^2 + (p+q)^2$. Therefore the information capacity of the reconstructed data of blind-SIM is given by

$$H_{\text{out}} = \frac{1}{2}(Nq^2 + (p+q)^2) \log_2(SNR_{\text{out}} + 1). \tag{S11}$$

Here, Nq^2 is the total number of diffraction-limited spots of reconstructed speckle patterns, and $(p+q)^2$ the number diffraction-limited spots of the reconstructed blind-SIM image. The fact that the output cannot contain more information than the input results in

$$H_{\text{out}}^{\text{max}} = H_{\text{in}} \tag{S12}$$

$$N p^2 \log_2(SNR_{\text{in}} + 1) = (Nq^2 + (p+q)^2) \log_2(SNR_{\text{out}}^{\text{max}} + 1). \tag{S13}$$

Random uncorrelated speckle pattern illumination allows a high oversampling that results in

$$\lim_{N \to \infty} SNR_{\text{out}}^{\text{max}} = (SNR_{\text{in}} + 1)^{\frac{p^2}{q^2}}. \tag{S14}$$

Here it is evident that as the illumination NA becomes higher compared to the detection NA, the $SNR_{\text{out}}^{\text{max}}$ drops rapidly due to the large number of high-resolution speckle patterns reconstructed from low-resolution images.

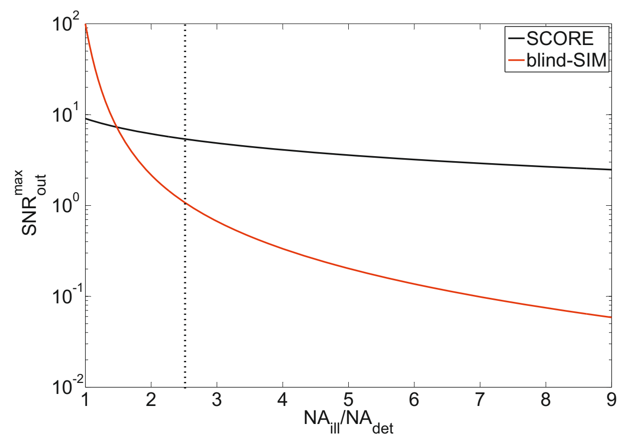

Fig. S9. Maximum signal-to-noise ratio of the SCORE and the blind-SIM images versus the NA ratio: The black line represents the SNR_{out} of SCORE. The red line represents the SNR_{out} of blind-SIM. The dashed vertical line shows the the NA ratio in our experiment.

Fig. S9 shows the comparison of the maximum possible SNR_{out} of SCORE to that of blind-SIM. We plotted the graph using equations S9 and S14 for a $SNR_{\text{in}} = 100$ for both methods which is realistic in experimental conditions. The SNR_{out} scaling law is different in each method. Blind-SIM has a higher SNR_{out} if the illumination NA is similar to the detection NA, which is the case when the same microscope objective is used for both illumination and detection. However, SCORE has higher SNR_{out} if the illumination NA is about 1.5 higher than the detection NA. In our case, we use a very high-NA scattering lens in the illumination $\text{NA}_{\text{ill}} = 2.4$ and a microscope objective in the detection with $\text{NA}_{\text{det}} = 0.95$. In this regime, SCORE has higher SNR_{out} compared to blind-SIM.

This simple information-theoretical analysis points out the regimes which each method can be expected to have the best performance.

REFERENCES

1. E. G. van Putten, D. Akbulut, J. Bertolotti, W. L. Vos, A. Lagendijk, and A. P. Mosk, "Scattering lens resolves sub-100

nm structures with visible light," Phys. Rev. Lett. **106**, 193905 (2011).

2. J. R. Fienup, "Phase retrieval algorithms: A comparison," Appl. Opt. **21**, 2758–2769 (1982).
3. J. W. Goodman, *Introduction to Fourier Optics* (Roberts & Company, Englewood, 2005).
4. L. Novotny and B. Hecht, *Principles of Nano-Optics* (Cambridge Univ. Press, Cambridge, U.K., 2006).
5. M. A. Neifeld, "Information, resolution, and space-bandwidth product," Opt. Lett. **23**, 1477–1479 (1998).